Inorganic Chemistry
Communication

Inorg. Chem. **2010**, *49*, 4759–4761 **4759**
DOI: 10.1021/ic100439n

Oxidation of Glutathione by $[Fe^{IV}(O)(N4Py)]^{2+}$: Characterization of an $[Fe^{III}(SG)(N4Py)]^{2+}$ Intermediate

Ashley A. Campanali, Timothy D. Kwiecien, Lew Hryhorczuk, and Jeremy J. Kodanko*

Department of Chemistry, Wayne State University, 5101 Cass Avenue, Detroit, Michigan 48202

Received March 5, 2010

The mechanism of glutathione (GSH) oxidation by a nonheme ferryl species has been investigated. The reaction of $[Fe^{IV}(O)(N4Py)]^{2+}$ (**1**) with GSH in an aqueous solution leads to the rapid formation of a green intermediate, characterized as the low-spin ferric complex $[Fe^{III}(SG)(N4Py)]^{2+}$ (**2**) by UV−vis and electron paramagnetic resonance spectroscopies and by high-resolution time-of-flight mass spectrometry. Intermediate **2** decays to form the final products $[Fe^{II}(OH_2)(N4Py)]^{2+}$ and the disulfide GSSG over time. The overall reaction was fit to a three-step process involving rapid quenching of the ferryl by GSH, followed by the formation and decay of **2**, which are both second-order processes.

Glutathione (GSH) is a ubiquitous tripeptide involved in many different aspects of cell growth and regulation (Figure 1). Arguably, its most important role is as an antioxidant, where it acts as a key player in defense and survival. GSH protects cells against oxidative stress by rapidly quenching reactive oxygen species, including hydroxyl radical and superoxide. This role is well understood.[1] In contrast, the reactivity of GSH with metal-based oxidants such as ferryls [iron(IV) oxo species], which are powerful oxidizing agents generated by heme[2,3] and nonheme enzymes,[4] has received much less attention.[5−7] This is worth investigating because GSH is thought to be the primary line of defense against detrimental ferryl species, such as ferryl myoglobin, in cells.[8] In this Communication, we report the reaction of GSH with a synthetic ferryl $[Fe^{IV}(O)(N4Py)]^{2+}$ (**1**).[9,10] Included are the characterization of a low-spin ferric species $[Fe^{III}(SG)(N4Py)]^{2+}$ (**2**), which is an intermediate in the process of GSH oxidation, and kinetic studies that have elucidated the overall reaction mechanism. This study has relevance to biology and the protection of cells by GSH against damage by ferryl compounds.

Previous studies in our laboratory[11] revealed that ferryl **1** is rapidly quenched by the cysteine derivative Ac-Cys-NHtBu in 1:1 H_2O/MeCN, which leads to the formation of a disulfide product. During data collection, the generation of a new green species with an absorbance maximum at 658 nm was observed by UV−vis spectroscopy after the disappearance of **1** (λ_{max} = 680 nm), which was present for ca. 1 h. However, only trace amounts of the species were observed, and the formation suffered from low reproducibility. Because this absorbance fell within the range of known S → Fe^{III} ligand-to-metal charge-transfer (LMCT) bands,[12,13] we surmised that the new species was likely a ferric thiolate. Therefore, we investigated the reactivity of related thiols with ferryl **1** and quickly settled upon GSH because the generation of an intermediate green species was highly reproducible and the reaction could be performed in an aqueous buffer, without the need for MeCN. Interestingly, many other thiols failed to form the green species, which may provide evidence for the structure of the green intermediate (vide infra).

The reaction of ferryl **1** with GSH was investigated in detail. To generate **1**,[14,15] $[Fe^{II}(N4Py)(MeCN)](ClO_4)_2$ (2 mM)[16] was dissolved in 100 mM acetate buffer (pH = 6.02) and treated with 2 equiv of aqueous peracetic acid, which led to the maximum generation of **1**, as judged by UV−vis spectroscopy. The reaction of **1** (1 mM) with GSH (5 mM) showed the rapid formation of a green intermediate with λ_{max} = 650 nm (< 45 s), clearly distinct from **1** (see Figure S2 in the Supporting Information), followed by a slower decomposition of the

*To whom correspondence should be addressed. E-mail: jkodanko@chem.wayne.edu.

(1) Hayes, J. D.; McLellan, L. I. *Free Radical Res.* **1999**, *31*, 273–300.
(2) Groves, J. T.; Haushalter, R. C.; Nakamura, M.; Nemo, T. E.; Evans, B. J. *J. Am. Chem. Soc.* **1981**, *103*, 2884–2886.
(3) Denisov Ilia, G.; Makris Thomas, M.; Sligar Stephen, G.; Schlichting, I. *Chem. Rev.* **2005**, *105*, 2253–2277.
(4) Krebs, C.; Fujimori, D. G.; Walsh, C. T.; Bollinger, J. M., Jr. *Acc. Chem. Res.* **2007**, *40*, 484–492.
(5) Galaris, D.; Cadenas, E.; Hochstein, P. *Free Radical Biol. Med.* **1989**, *6*, 473–478.
(6) Romero, F. J.; Ordonez, I.; Arduini, A.; Cadenas, E. *J. Biol. Chem.* **1992**, *267*, 1680–1688.
(7) Puppo, A.; Monny, C.; Davies, M. J. *Biochem. J.* **1993**, *289*, 435–438.
(8) D'Agnillo, F.; Alayash, A. I. *Free Radical Biol. Med.* **2002**, *33*, 1153–1164.
(9) Que, L. *Acc. Chem. Res.* **2007**, *40*, 493–500.
(10) Nam, W. *Acc. Chem. Res.* **2007**, *40*, 522–531.
(11) Abouelatta, A. I.; Campanali, A. A.; Ekkati, A. R.; Shamoun, M.; Kalapugama, S.; Kodanko, J. J. *Inorg. Chem.* **2009**, *48*, 7729–7739.
(12) Koch, S.; Tang, S. C.; Holm, R. H.; Frankel, R. B.; Ibers, J. A. *J. Am. Chem. Soc.* **1975**, *97*, 916–918.
(13) Kennepohl, P.; Neese, F.; Schweitzer, D.; Jackson, H. L.; Kovacs, J. A.; Solomon, E. I. *Inorg. Chem.* **2005**, *44*, 1826–1836.
(14) Kaizer, J.; Klinker, E. J.; Oh, N. Y.; Rohde, J.-U.; Song, W. J.; Stubna, A.; Kim, J.; Münck, E.; Nam, W.; Que, L., Jr. *J. Am. Chem. Soc.* **2004**, *126*, 472–473.
(15) Sastri, C. V.; Seo, M. S.; Park, M. J.; Kim, K. M.; Nam, W. *Chem. Commun.* **2005**, 1405–1407.
(16) Roelfes, G.; L., M.; Leppard, S. W.; Schudde, E. P.; Hermant, R. M.; Hage, R.; Wilkinson, E. C.; Que, L., Jr.; Feringa, B. L. *J. Mol. Catal. A: Chem.* **1997**, *117*, 223–227.

Published on Web 05/06/2010

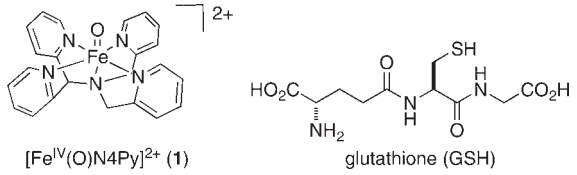

Figure 1. Structures of **1** and GSH.

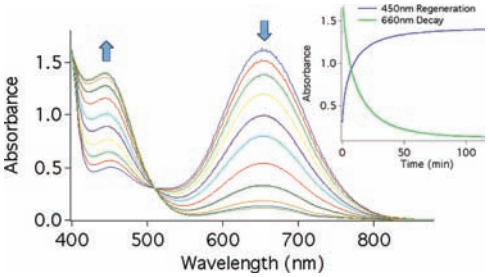

Figure 2. Reaction of **1** (1 mM) with GSH (5 mM); UV−vis data for the decay of the intermediate with λ_{max} = 650 nm and the regeneration of $[Fe^{II}(OH_2)(N4Py)]^{2+}$ at λ_{max} = 450 nm. Inset: Time course decay of λ_{max} = 650 nm and time course regeneration of λ_{max} = 450 nm.

green species, which coincided with the regeneration of $[Fe^{II}(OH_2)(N4Py)]^{2+}$ (λ_{max} = 450 nm; Figure 2). The yield of $[Fe^{II}(OH_2)(N4Py)]^{2+}$ was 89% at the end of the reaction, based on an absorbance measurement using its extinction coefficient under these conditions (1620 M^{-1} cm^{-1}). An isosbestic point was observed at 510 nm, indicating that there were no long-lived intermediates in the conversion of the green species into the Fe^{II} product. Following the decay, the yield of oxidized disulfide GSSG, based on GSH consumption, was determined by Ellman's reagent to be 90 ± 20% based on **1**. The formation of GSSG was verified by electrospray ionization mass spectrometry (MS). No other oxidized GSH products, such as sulfenic, sulfinic, or sulfonic acids, were detected.

Control experiments were performed to determine if the green intermediate contained iron, GSH, and N4Py. The absorption at λ_{max} = 650 nm, indicative of a $S \rightarrow Fe^{III}$ LMCT band rather than a d−d transition based on its extinction coefficient (vide infra), was not observed in control experiments with $Fe^{II}(ClO_4)_2$ or $Fe^{III}(ClO_4)_3$ salts alone, which suggests a role for the ligand N4Py in the complex. Furthermore, when the aliphatic or aromatic thiols EtSH or PhSH were treated with **1**, no species with an absorbance band in the visible region were detected by UV−vis spectroscopy. The reaction of GSH with $[Fe^{II}(N4Py)(MeCN)](ClO_4)_2$ did not show the rapid formation of an absorption band at 650 nm, confirming a role for **1** in the formation of the green species.[17] However, if aqueous solutions of $Fe^{II}(N4Py)(MeCN)](ClO_4)_2$ were allowed to oxidize in air before GSH was added, the green species was observed to generate rapidly, which is consistent with the reaction of a ferric intermediate with GSH leading to the formation of the green species, as indicated in the proposed mechanism (vide infra). After determination of what was responsible for the formation of the green intermediate, other characterization data were collected.

(17) The oxidation of GSH by $[Fe^{II}(N4Py)]^{2+}$ and the formation of **2** will occur under aerobic conditions, but it is a much slower process; see Figure S3 in the Supporting Information.

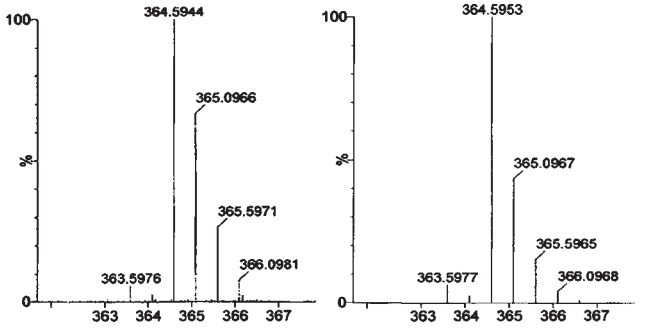

Figure 3. High-resolution TOF-MS of **2** with *m*/*z* 364.5944 (left) and a calculated fit (right).

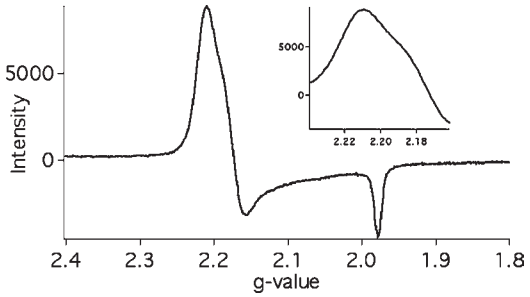

Figure 4. X-band EPR spectra from the reaction of **1** (1 mM) with GSH (5 mM). The sample was frozen in liquid N_2 1 min after mixing. Inset: Expansion of the spectrum showing a shoulder at g = 2.19. Experimental conditions: temperature, 120 K; microwaves, 1.0 mW at 9.34 GHz; modulation, 2.0 G, receiver gain, 14 000.

The reaction of **1** and GSH was followed by MS. At early time points, the high-resolution time-of-flight (TOF)-MS spectrum displayed a prominent ion cluster with a dominant peak at *m*/*z* 364.5944. This cluster displayed an isotopic distribution that fit with the molecular formula $[Fe^{III}(SG)(N4Py)]^{2+}$ (denoted as **2**, Figure 3). In this dication, the ligand derived from GSH was treated as a monoanion (i.e., GSH − H^+), as would be expected if the thiolate of GSH were deprotonated and bound to Fe^{III} and the rest of the GSH ligand was formally neutral. In addition, a separate ion cluster was observed with a dominant peak at *m*/*z* 728.1821 (see the Supporting Information), which was fit to the formula $[Fe^{III}(SG)(N4Py)]^{+}$, where the GSH portion of the species was treated as a dianion (i.e., GSH − $2H^+$), presumably because of deprotonation of both carboxylate groups and protonation of the amine on the terminus of GSH. After 1 h at room temperature, these ion clusters gave way to a major ion cluster with *m*/*z* 220.418, which is consistent with the molecular formula $[Fe^{II}(OH_2)(N4Py)]^{2+}$.

The green intermediate **2** was characterized by electron paramagnetic resonance (EPR) spectroscopy. Spectra were acquired at multiple time points during the formation and decay of **2** (see the Supporting Information). A new species was detected with *g* values of 2.17 and 1.98 (Figure 4), which formed and then decayed on the same time scale as the absorption band with λ_{max} = 650 nm, consistent with its assignment as **2**. The EPR spectrum in Figure 4 shows an apparent shoulder for the resonance at 2.17, suggesting that a third resonance with a slightly higher *g* value may be present but is not resolved, which would indicate rhombic rather than axial symmetry. In either case, the EPR spectrum in Figure 4 is consistent with intermediate **2** being a low-spin Fe^{III} species

because the data agree well with the related species $[Fe^{III}(X)(N4Py)]^{2+}$ (X = OH, OOH).[18]

To probe the mechanism of GSH oxidation further, kinetic data were collected for the reaction of **1** (1 mM) with variable concentrations of GSH (5−25 mM), and the UV−vis data were fit using the kinetic modeling software *Dynafit*.[19] Because of the fast generation of **2** (< 1 min to reach completion), a stopped-flow apparatus was employed. Under all conditions, greater than 50% decay of the ferryl **1** was complete within the deadtime of mixing, which places a lower limit for the rate constant of ferryl quenching (k_1) by GSH at $1 \times 10^4\ M^{-1}\ s^{-1}$. On the basis of previous studies with Ac-Cys-NHtBu and our visual observation of a transient yellow color within the first several seconds of the reaction, the formation of the ferric intermediate $[Fe^{III}(OH)(N4Py)]^{2+}$ (labeled **I** in eqs 1 and 2) is proposed for this first step.[20] The next two steps of the reaction, the formation and decay of the green intermediate **2**, were evaluated using several proposed mechanisms (see the Supporting Information for further details). First- and second-order processes were considered for both steps, and the data fit best to the following reaction scheme involving a second-order reaction between GSH and **I** [$k_2 = 14.3(1)\ M^{-1}\ s^{-1}$, eq 2], followed by a second-order decomposition of **2** that had zero kinetic order in GSH [$k_3 = 1.68(1)\ M^{-1}\ s^{-1}$, eq 3]. A value for $\varepsilon_{650} = 1870\ M^{-1}\ cm^{-1}$ was calculated for **2** by extrapolating the linear portion of $1/A$ vs t to $t = 0$, which agreed well with the response factor that was optimized by the *Dynafit* software.

$$[Fe^{IV}(O)(N4Py)]^{2+}\ (\mathbf{1}) + GSH \rightarrow \mathbf{I} + \frac{1}{2}GSSG \quad (k_1) \quad (1)$$

$$\mathbf{I} + GSH \rightarrow [Fe^{III}(SG)(N4Py)]^{2+}\ (\mathbf{2}) + H_2O \quad (k_2) \quad (2)$$

$$2[Fe^{III}(SG)(N4Py)]^{2+}\ (\mathbf{2}) + 2H_2O \rightarrow 2[Fe^{II}(OH_2)(N4Py)]^{2+} + GSSG \quad (k_3) \quad (3)$$

Given the observed second-order decay of **2**, homolysis of the Fe^{III}−SG bond and dimerization of two $GS^{\bullet}$ radicals to form GSSG are proposed as the mechanism for eq 3.[21] The N-rich ligand set of N4Py may provide an extra driving force for this homolysis step by favoring the Fe^{II} state over Fe^{III}. However, Fe−S bond homolysis is likely to be reversible in an aqueous solvent, as indicated by the faster rate of decay that was observed for **2** in 1:1 H_2O/MeCN versus an aqueous buffer alone (see the Supporting Information). In the mixed solvent where MeCN is in large excess, MeCN may trap the $[Fe^{II}(N4Py)]^{2+}$ intermediate and make homolysis irreversible by forming the stable low-spin ferrous complex $[Fe^{II}(MeCN)(N4Py)]^{2+}$. However, other effects, such as a change in the dielectric constant of the solvent medium, as well as other reaction mechanisms, cannot be ruled out at this point.

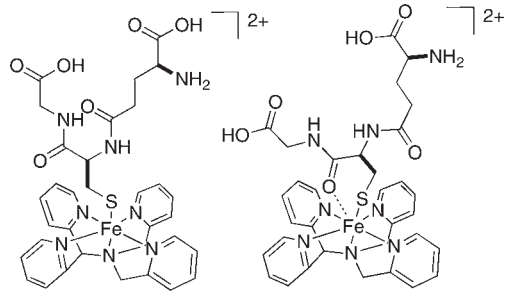

Figure 5. Possible structures of **2** showing η^1 coordination by the GS^- thiolate or an alternative chelate structure.

A green intermediate was observed in the reaction of **1** with GSH and not with other thiols. Several models for the structure of **2** are possible (Figure 5), including the simplest model that would involve η^1 binding of the GS^- thiolate to an octahedral Fe^{III} center. Thiolate binding to the iron center is supported by the absorption band at 650 nm. However, it is possible that additional groups of GSH, such as the carbonyl of the Cys residue, are coordinating as well. The existence of a chelate structure is supported by the fact that coordination numbers higher than 6 have been observed for N4Py complexes[18] and because GSH and not simple thiols form the green intermediate. Future studies will be needed to understand the coordination mode of **2**.

In conclusion, the kinetics of GSH oxidation by the ferryl **1** has been investigated, and the intermediate ferric thiolate **2** has been identified by EPR, high-resolution TOF-MS, and UV−vis spectroscopy. Compound **2** is the first example of a sulfur donor bound to the iron center of an N4Py complex. The rapid quenching of ferryl **1** and subsequent oxidation of GSH are relevant to biology and the protection of cells against damage by metal-based oxidants. Further studies concerning the oxidation of GSH and other biologically relevant thiols are underway in our laboratory.

Acknowledgment. We thank Wayne State University for its generous financial support of this research.

Supporting Information Available: Experimental procedures, UV−vis, MS, and EPR spectra, and kinetic fits. This material is available free of charge via the Internet at http://pubs.acs.org.

(18) Roelfes, G.; Vrajmasu, V.; Chen, K.; Ho, R. Y. N.; Rohde, J.-U.; Zondervan, C.; la Crois, R. M.; Schudde, E. P.; Lutz, M.; Spek, A. L.; Hage, R.; Feringa, B. L.; Muenck, E.; Que, L., Jr. *Inorg. Chem.* **2003**, *42*, 2639–2653.

(19) Kuzmic, P. *Anal. Biochem.* **1996**, *237*, 260–273.

(20) Collins, M. J.; Ray, K.; Que, L., Jr. *Inorg. Chem.* **2006**, *45*, 8009–8011.

(21) Second-order decays have been noted for copper(II) thiolates of cysteine. See: Baek, H. K.; Holwerda, R. A. *Inorg. Chem.* **1983**, *22*, 3452–3456.